Dynamical Observation of Structural Transition of Polymers Using an X-ray Diffraction System with Imaging Plates. 1. Reversible Helix/Helix Transformation of Poly(vinylcyclohexane)

Yukihiro Nishikawa,† Syozo Murakami, Shinzou Kohjiya, and Akiyoshi Kawaguchi*

The Institute for Chemical Research, Kyoto University, Uji, Kyoto 611, Japan

Received December 4, 1995; Revised Manuscript Received May 2, 1996[⊗]

ABSTRACT: Two different crystalline forms were caused by drawing an unoriented isotactic poly(vinylcyclohexane) film, Form I and Form II, depending on the drawing temperature. Form II was changed into Form I thermally and Form I was converted into Form II by drawing. This reversible phase transformation was followed by dynamical X-ray observation. The X-ray measurements were carried out with an X-ray diffraction system with imaging plates, which was designed to record X-ray diffraction patterns over a series of short time spans while the samples were being heated or drawn. When samples were drawn at temperatures below about 110 °C, Form I was produced, and Form II was formed at higher temperatures. Through dynamical observations with the X-ray diffraction system, it was found that Form I occurred at an early stage of drawing independently of the drawing temperature and that the crystalline form was changed into Form II by further drawing at high temperatures, e.g., 130 °C. Form II was transformed into Form I by heat treatment at temperatures above 248 °C. When the heat-treated sample of Form I was drawn at, e.g., 133 °C, the crystalline form was transformed into Form II. Thus, the transformation of Form II into Form I occurred thermally at temperatures above 248 °C and the inverse transformation was induced by applying the stress at temperatures above about 110 °C.

Introduction

In processing of crystalline polymers, nucleating agents are important to produce highly qualified products. There are various kinds of inorganic and organic nucleating agents, and further effective ones are being searched for. It has been found that isotactic poly(vinylcyclohexane) (iPVCH, $-(CH_2CH(C_6H_{11})_n-$) acts effectively as a nucleating agent in the processing of isotactic polypropylene (iPP) to give rise to highly transparent iPP films.[1] A polymeric nucleating substance is more appropriate because it is not bled out after the iPP films are processed and is able to be mixed in iPP in the process of its polymerization. There are two reported modifications of iPVCH crystal structures: the tetragonal form comprising chains of a 4/1 helix (Form I)[2] and a form with a 24/7 helix (Form II).[3] The modification produced is variable depending on the treatment and the external environment, e.g., temperature. From the industrial point of view of enhancing the nucleating effect of iPVCH on the processing of iPP, it is important to know which form exhibits a more effective nucleating performance. Here, as a starting point, the conditions for producing either of the two forms are studied.

While various types of highly sensitive recording media of X-ray intensity have been developed, recently imaging plates (IPs) have been spotlighted and utilized in the field of science, e.g., for a detector of X-rays, electrons, or neutrons. IPs have the advantage that they are two-dimensional, highly sensitive media and may be used over and over for recording and deleting data.[4] Presently, the changes of X-ray diffraction patterns in the transient process of structural changes of polymers are able to be recorded as a time series of a short period by using a system in which the imaging plates are combined with a powerful X-ray source, for example, as a time series of 0.1 s time span in combination with synchrotron orbital radiation.[5] In cooperation with MAC Science Co. Ltd., Japan, we designed and constructed an X-ray diffraction system (sold with a commercial name DIP220) in combination with IPs and a rotating-anode X-ray generator, with which X-ray diffraction patterns are able to be recorded sequentially as a time series of as short a time span as 10 s. Using this system, we found that the transformation of the orthorhombic phase to a monoclinic phase of ultrahigh molecular weight polyethylene occurs while it is being drawn at a temperature below about 100 °C,[6] and we revealed that the double orientation is caused by uniaxial drawing of poly(ethylene naphtharate).[7] In the present paper, we show the crystal/crystal transition of iPVCH by drawing and by heating, accompanying the helix/helix transformation of iPVCH chain, which was disclosed by *in-situ* observation with the newly constructed X-ray diffraction system.

Experimental Section

The molecular weight of the iPVCH used was about 2.4×10^5 (the polymer was supplied by Sumitomo Chemical Co. Ltd.). iPVCH was first dissolved in tetrachloromethane (CCl_4, a good solvent) at a concentration of 1%. A 0.5 mm thick iPVCH film was made by evaporating the solvent at room temperature. The film was drawn at various temperatures, and then X-ray diffraction patterns were taken *in situ* by using the X-ray diffraction system while the film was drawn and heated. In the present apparatus, a heatable sample chamber was used for measuring at high temperatures, and the force imposed on a sample was measured with a drawing device attached to it. The setup and use of the X-ray diffraction system and the drawing device are described in refs 6 and 7. However, the system is not sufficiently well designed so as to keep the temperature uniform inside the chamber. Thus, the sample temperature indicated below is of that part through which the incident beams of X-ray pass and was measured by a thermocouple attached there.

* To whom correspondence should be addressed. Present address: Department of Chemistry, Faculty of Science and Engineering, Ritsumeikan University, Kusatsu, Shiga 525, Japan.

† Present address: Hashimoto Project ERATO JRDC, Keihanna-plaza, 1-7 Hikaridai, Seika, Kyoto-fu 619-02, Japan.

⊗ Abstract published in *Advance ACS Abstracts,* July 1, 1996.

S0024-9297(95)01789-X CCC: $12.00

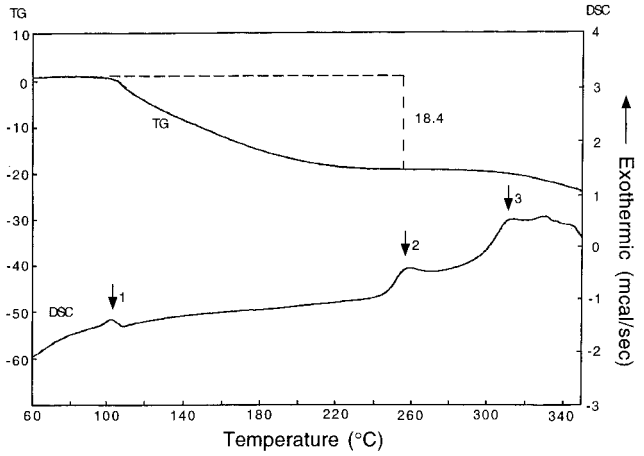

Figure 1. TG and DSC curves of an as-cast iPVCH film, measured at a heating rate of 10 °C/min.

Table 1. Experimental Scheme

PVCH powder
↓ cast from 1% tetrachloromethane solution
as-cast Film
• DSC/TG (figure 1).
(Run1) • Dynamical X-ray obervation during heating up to 270°C (figure 2).
(Run2) • Dynamical X-ray observation during drawing at 112°C (figure 6).
(Run3) • Dynamical X-ray observation during drawing at 154°C (figure 7). Stress was also measured in the same run (figure 8A).
(Run4) • Stress-Strain measurement at 150°C (figure 8B).
→ drawn at 100°C (figure 4A)
• DSC (figure 3A)
(Run5) • X-ray obervation during heating up to 270°C (The experimental results are not present because there was no change in diffraction patterns).
→ drawn at 130°C (figure 4B)
• DSC (figure 3B)
(Run6) • X-ray obervation during heating up to 270°C (figure 5).
→ annealed at 250°C (figure 4C)
• DSC (figure 3C)
(Run7) • X-ray observation during drawing at 130°C (figure 9).

Differential scanning calorimetric (DSC) measurements were also carried out by using the Rigaku TAS 100 system. The experimental scheme is shown in Table 1.

In the X-ray diffraction system with IPs, intensity data are read out as digital values so that they are readily processed with a personal computer (PC). Substantially, the patterns are displayed and processed on the CRT of the PC. The image processing program was written by ourselves in FTN77, which is a special FORTRAN compiler developed for PCs by Salford Software, U.K. The image processing program and its applicability will be described elsewhere.

Results and Discussion

Thermal Behavior of As-Prepared and Oriented iPVCH. Figure 1 shows a DSC−TG thermogram of an as-cast, unoriented iPVCH film, which was measured at a heating rate of 10 °C/min. There are three exothermic peaks in the DSC curve. The TG curve shows that the weight of the iPVCH film gradually decreases with increasing temperature and levels off with an 18.4% loss of weight at about 250 °C and with further heating, gradually decreasing again. The first decrease in weight shows that the solvent is still contained in original films and is removed with increasing temperature; the second decrease in weight is due to decomposition of iPVCH. The weight of the as-cast film starts decreasing at the temperature close to that

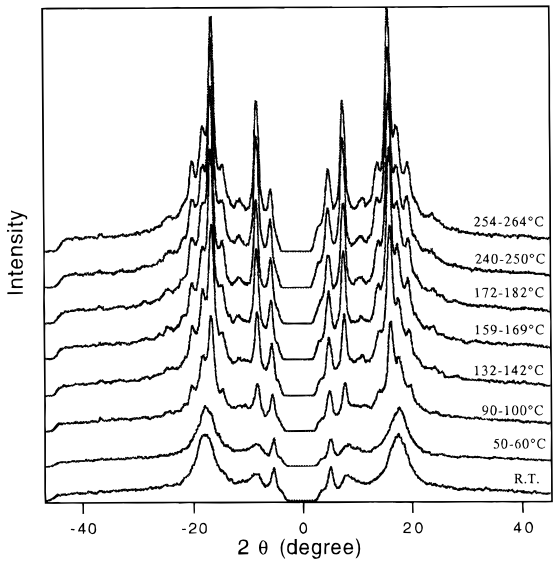

Figure 2. Changes of wide-angle X-ray diffraction profiles while an as-cast, unoriented iPVCH film was heated at a heating rate of 1 °C/min. The exposure time of individual patterns was 10 min, and hence they were recorded as an accumulation of patterns which were changing during the time interval, i.e., while the sample was heated by 10 deg. The diffraction profiles were taken from the pictures recorded *in situ* with IPs and processed by the image processing program.

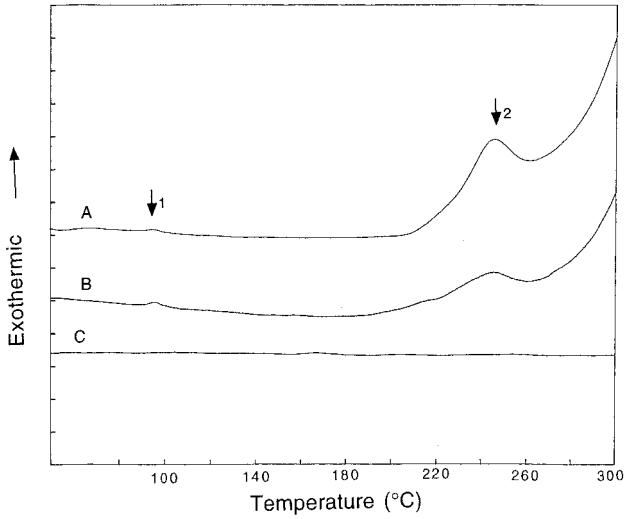

Figure 3. DSC thermograms of (A) a sample prepared by drawing a cast film at 100 °C, (B) a sample prepared by drawing it at 130 °C, and (C) the sample after sample B was heat-treated at 250 °C (see text).

of the first DSC exothermic peak, ~100 °C. Since the boiling point of CCl_4 is 76.7 °C, however, it is clear that the first exotherm observed at about 100 °C is not due to "evaporation of CCl_4". We see thus that the first exotherm accompanies evolution of CCl_4 from the film, being closely related to the increase of molecular motion of iPVCH, e.g., the glass transition temperature (110−150 °C).[8] Though not assessed quantitatively, the peak temperature of the exotherm changes from sample to sample, probably because the content of the solvent differs among the samples. Here, it is to be noted that the weight continues decreasing up to the second exothermic peak, although the rate is reduced with temperature. The third exotherm is attributed to the decomposition of chains.

Figure 2 shows a series of wide-angle X-ray diffraction patterns (WAXDPs) which were recorded using the

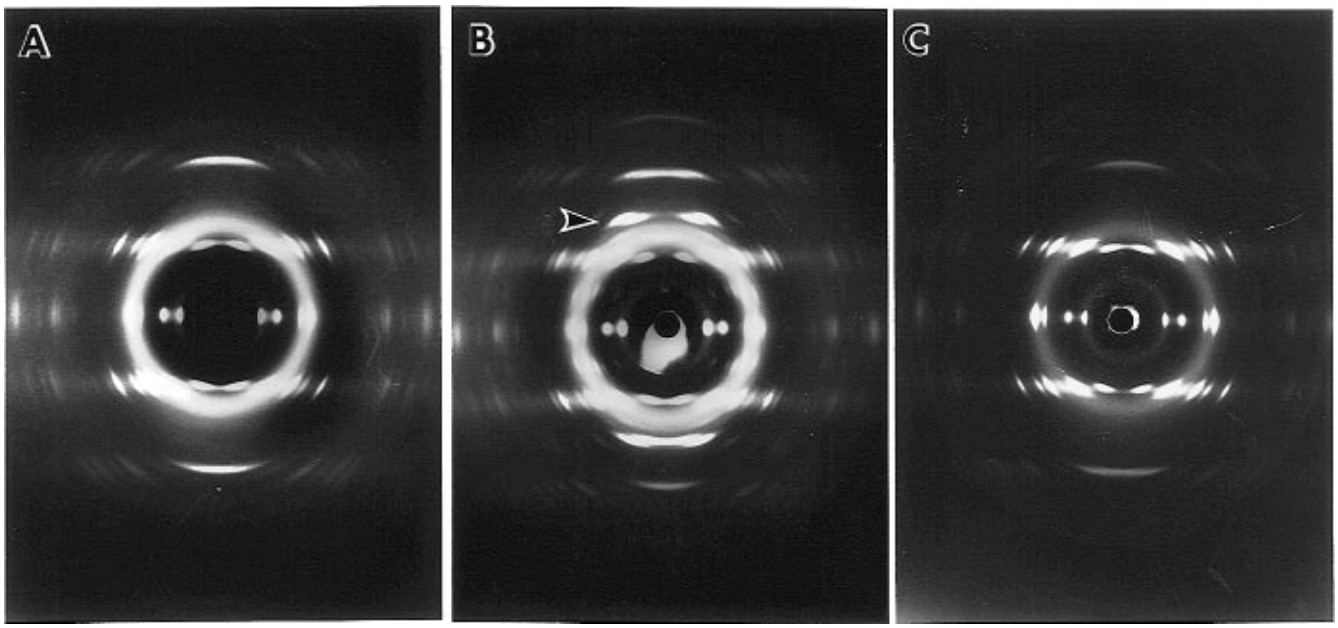

Figure 4. WAXDPs of samples A, B, and C in Figure 3, which were photographed on X-ray films with a cylindrical camera.

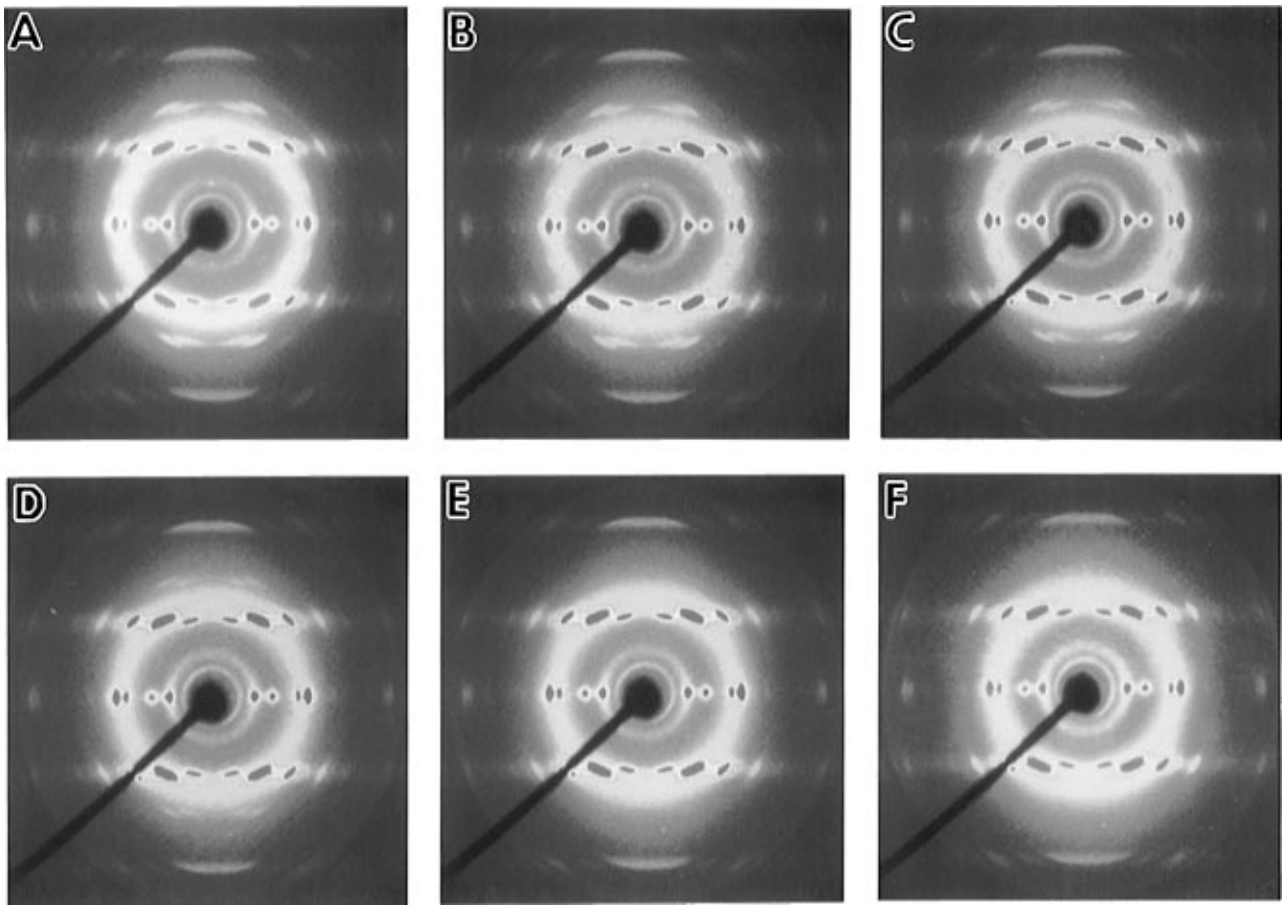

Figure 5. WAXDPs of sample B which were taken with the X-ray diffraction system at fixed temperatures: (A) 220, (B) 230, (C) 240, (D) 240, (E) 250, and (F) 300 °C. The exposure time of individual patterns is 10 min. All the patterns are photographed from the pictures which were displayed on a CRT in the form of patterns of a cylindrical camera by image processing.

X-ray diffraction system with IPs while an as-cast, unoriented sample was being heated (see run 1 in Table 1, and so forth). The temperature range indicated in Figure 2 covers that of the first exotherm peak in the DSC of Figure 1. Before the exotherm, the WAXDP has broad halos only, indicating that the sample is amorphous. As the temperature is increased above the peak temperature, sharp crystalline reflections appear. This means that the crystallization proceeds with removal of the solvent.

Three kinds of drawn samples were prepared: a film drawn at 100 °C to the draw ratio of about 5 (sample A), a film at 130 °C to the draw ratio of about 5 (sample B), and an oriented sample after a drawn sample (sample B) was heated once to 250 °C (sample C). In Figure 3, DSC themograms of samples A, B, and C are

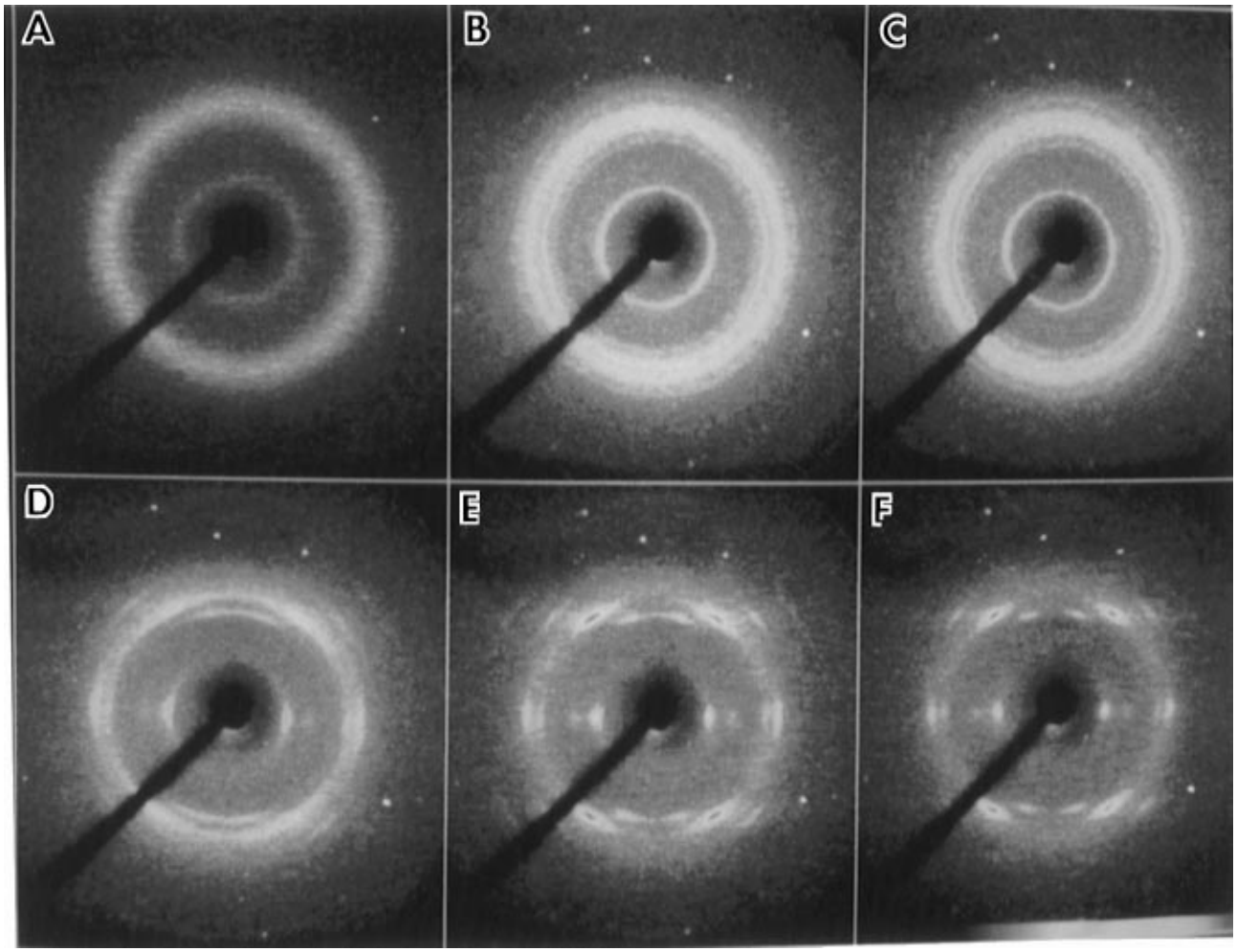

Figure 6. Changes of WAXDPs when a cast film of iPVCH of the length 2 cm and width 5 mm was drawn at a drawing rate of 2 mm/min at 112 °C. Individual patterns were taken with an exposure time of 2 min: (A) at room temperature before heating; (B) before drawing at 112 °C; (C) 0.10 MPa; (D) 0.34 MPa; (E) 2.61 MPa; (F) 4.78 MPa. Hence, they were recorded as an accumulation of patterns which were changing during the time interval while the sample was being drawn. All the patterns are photographed from the pictures which were displayed on a CRT in the form of patterns of a cylindrical camera.

shown as curves A, B, and C, respectively, obtained at a heating rate of 10 °C/min. In curves A and B, two exothermic peaks are observed. The peak temperature of the first exotherm just corresponds to that of the first exotherm in Figure 1. The second exotherms of samples A and B are observed at the same temperature, i.e., 248 °C, as the second exotherm in Figure 1, and the amounts of exothermic heat are evaluated at 26.7 and 7.68 J/g, respectively. The second exotherm is seen in both curves A and B, but not in curve C. As the melting temperature is reported to be 370 °C,[3,8] the exotherm suggests that a crystal/crystal transition occurs. WAXDPs of these samples taken at room temperature are compared in Figure 4. Figures 4A and 4C show that the crystalline modification is Form I. Figure 4B indicates that a Form II exists, but it is not clear whether it is Form II only or both forms coexist. The reflections on the layer line indicated by the arrow in Figure 4B are characteristic of Form II (referred to as *the characteristic layer line* below). Clearly, the crystalline form changes from Form II to Form I after as-drawn films are annealed at temperatures above 248 °C, and hence the second exothermic peak at 248 °C of DSC curves A and B in Figure 3 is caused by the crystal/crystal phase transition. Noether et al. reported that this phenomenon occurs in the temperatures range 240−260 °C.[3] This is supported by the DSC curve C in Figure 3 since there is no exo- or endotherm at this temperature. By using the present X-ray diffraction system, we actually followed the changes of WAXDPs while the sample with the crystalline phase of Form II was being heated, exceeding the exothermic peak temperature. Figure 5 shows a series of X-ray diffraction patterns thus observed, covering the temperature range of the second exotherm of the DSC curve B of Figure 3 (run 6). The reflections of the characteristic layer line start to reduce in intensity around 240 °C and disappear at 260 °C. It is thus clearly proven that the exotherm is due to the phase transformation from Form II to Form I. In conclusion, we point out the following.

(1) As seen in Figure 4, the crystalline phase is Form I when an unoriented film is drawn at 100 °C, and Form II when drawn at 130 °C. The limiting drawing temperature where Form II forms is about 110 °C.

(2) Sample A also exhibits the second exotherm, although it has the crystalline phase of Form I.

(3) The amorphous halo is very intense in Figures 4A and 4B and becomes weak by heat treatment above the second exothermic peak temperature, as seen in Figure 4C.

Difference of Crystalline Form by Drawing Temperature. In Figure 4, we see that the crystalline form of drawn samples differs depending on the drawing temperature. We followed dynamically the drawing behavior of unoriented iPVCH by using the X-ray diffraction system with IPs; the X-ray diffraction pat-

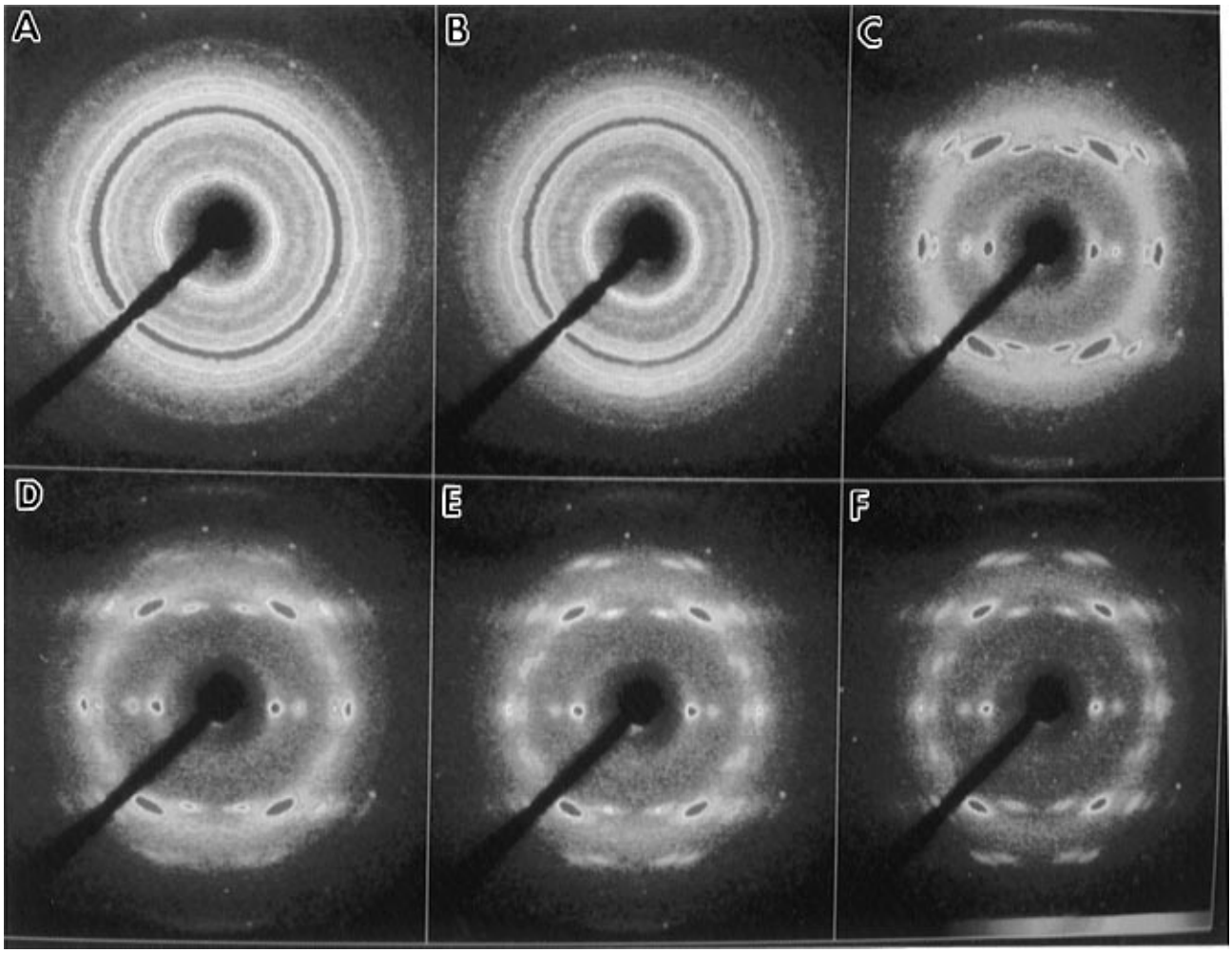

Figure 7. Changes of WAXDPs when a cast film of iPVCH of length 2 cm and width 5 mm was drawn at a drawing rate of 2 mm/min at 154 °C: (A) no stress; (B) 1.31 MPa; (C) 2.57 MPa; (D) 2.98 MPa; (E) 4.07 MPa; (F) after stress is removed. All the other experimental and analytical procedures are the same as in Figure 6.

terns were recorded as a time series of a short period of time while an as-cast iPVCH film was being drawn. The changes in force imposed on the sample and in its length were measured together as drawing proceeded. Figure 6 shows a series of X-ray diffraction patterns taken during drawing at 112 °C (run 2). Originally, they were taken as a time series, and the times at which they were recorded are converted to the applied stress in referring to the stress−time curve. In Figure 6C, where a stress of 0.1 MPa is applied, the molecular orientation starts, and with further drawing, the pattern is changed into a fiber pattern. During drawing, necking deformation occurs in this sample, and hence the draw ratio has no substantial meaning. Accordingly, instead of the draw ratio, we introduce the stress applied to the sample as a parameter so that it is more convenient to correlate the mechanical behavior with the molecular or crystalline structure. The degree of molecular orientation increases as the sample is drawn, but the reflections on the characteristic layer line of Form II do not appear during drawing. The crystalline form remains Form I through the entire drawing process. We must notice here the following: From the X-ray diffraction pattern (shown in Figure 2), it is not made clear which crystalline form the original unoriented iPVCH takes, Form I or II, because we cannot identify in the ring pattern the very reflections that characterize Form I or Form II. The DSC curve suggests that it is probable that the crystalline phase is Form II because it exhibits the large exothermic peak at 248 °C. However, we cannot ignore the fact that the DSC curve B in Figure 3 shows the exothermic peak even though the crystalline form is Form I.

Figure 7 shows the change of X-ray diffraction patterns which were taken serially while an unoriented film was being drawn at 154 °C at a drawing rate of 2 mm/min (run 3). Through necking deformation at a stress of 1.31 MPa, the Debye−Scherrer ring pattern is rather sharply changed into a fiber pattern. The crystalline form of the drawn sample is Form I because Figure 7C shows no reflections on the characteristic layer line of Form II. When the oriented film was drawn further, the molecular orientation proceeds, and concurrently the reflections on the Form II characteristic layer line appear at a stress of 2.98 MPa. The reflections become more and more intense with the increase of stress. Here, we know that the molecular orientation proceeds at an early stage of drawing while the crystalline phase of Form I remains. Accordingly, the Form II is not due to the fact that the sample was drawn at high temperatures but is caused when higher stress is applied. As the issue (1) in the last section on the basis of the static observations by X-ray diffraction, we describe that there is a difference in deformation behavior by drawing between at low temperature and at high temperatures. However, Form I only rises at an early stage of drawing, i.e., at a stage of drawing of low stress, independently of temperature. We thus expect that in the case of the drawing at a lower

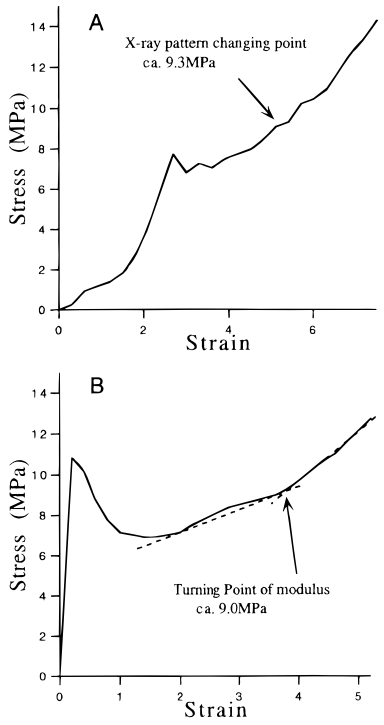

Figure 8. Stress−strain curves when an as-cast film was drawn: (A) transferred from the force−length data measured by the present X-ray diffraction system at 154 °C (corresponding to Figure 7) and (B) measured at 150 °C by a testing machine equipped with a temperature-controllable sample chamber.

temperature, this transformation would take place when a higher stress is applied. Unfortunately, the sample was broken down during drawing at a lower temperature, so that the limiting temperature where drawn film of Form II was obtained is about 110 °C. This fracture behavior at low temperatures without producing Form II might be inherent to the molecular structure and the texture.

Stress-Induced Form I/Form II Transition. As described in the Experimental Section, the temperature is not uniform over the entire sample because a temperature gradient inevitably arises in the drawing device used in the X-ray diffraction system. Though the changes in sample length were able to be recorded with the device together with the applied forces, we could not convert the as-measured force−elongation curves to stress−strain curves due to inhomogeneous deformation of the sample. These experimental ambiguities are corrected in the procedure described below. Using the cross-section of the undrawn sample as a standard, the apparent stress was evaluated. WAXDPs in Figures 6 and 7 are labeled with the thus obtained stress as an indicator. Since the sample was deformed inhomogeneously, we accessed the true stress as follows: reliable stress−strain curves were measured by using a testing machine which was equipped with a temperature-controllable heating chamber. Two stress−strain curves are compared in Figure 8: one is transferred from the data obtained by the X-ray diffraction experiment, i.e., from the data corresponding to Figure 7 (Figure 8A), and the other by the testing machine (run 4) (Figure 8B). In the case of X-ray diffraction, the forces were measured accurately. By comparing the stress of Figure 8A with that of Figure 8B, we can estimate the real strain during drawing in the X-ray diffraction work. In these curves, the stress was calculated using the cross-section of the drawn sample, i.e., the final cross-section after being drawn, not that before drawing. This calculation is useful to compare the results with those of Figure 9, where the drawn and annealed sample was redrawn, because the length of the sample suddenly increases up to the draw ratio of about 4 through necking in Figure 8 and the cross-sectional area decreases to the value corresponding to that of final sample. From Figure 8A, it is found that the stress at which the WAXDP changes to give reflections on the characteristic layer line is 9.3 MPa (corresponding to 2.98 MPa in Figure 7D and recalculated with it on the basis of the final cross-section). In Figure 8B, the slope of the stress−strain curve increases markedly at a stress of 9.0 MPa. This value just corresponds to the stress where the crystal phase changes in Figure 8A. The good agreement of both stresses means that the change of stress is caused by a change in the conformation of the molecular chain; in other words, the helical conformation can be changed with stress.

Once the sample is heat-treated at a temperature above 248 °C, only Form I exists: Form II is thermally transformed into Form I. We examined the transformation behavior (Form I to Form II) of the thus heat-treated film of Form I by drawing. Figure 9 shows a series of WAXDPs of the sample which were taken with an exposure time of 10 min under the indicated constant stress (run 7). Of course, no characteristic layer line is observed in Figure 9A under no stress. When a stress of 12.8 MPa is applied, the reflections on the characteristic layer line are very faintly detectable (see Figure 9D). With further increase of stress, the reflections become intense, showing the progress of transformation of Form I into Form II. Figure 9F shows the WAXDP of the sample after the stress is removed. While the sample relaxed at the temperature, there is no symptom in the WAXDP to show the reverse transformation of Form II into Form I. The stress needed to transform Form I into Form II differs between Figure 7 and Figure 9. This implies that the stress to cause the transformation depends on temperature; 12.8 MPa at 133 °C and 9.3 MPa at about 150 °C (in the case of Figure 9, the cross-section near the part through which X-ray beams passed was used).

Crystal Structure of iPVCH. As mentioned above, there are two crystalline modifications in iPVCH[2,3]: Form I has a tetragonal unit cell with $a = b = 2.199$ nm and $c = 0.643$ nm and comprises the chains of the 4/1 helix, and Form II is also tetragonal with cell dimensions $a = b = 2.048$ nm and $c = 4.458$ nm and its chain conformation is a 24/7 helix.[3] However, the mode of packing of chains in the unit cells and the actual helical conformation of both chains are not always detailed. Here, the findings of the crystal structures of iPVCH are outlined and their details will be described elsewhere.

(1) Form I. As a result of analyses of the WAXDPs of a well-oriented sample, the cell dimensions and the crystal system of Form I are the same as mentioned above, and the space group and molecular conformation are also found to be $I4_1/a$ and the 4/1 helix as shown in refs 2 and 3. Though the number of parameters defining the molecular conformation and the position and orientation of chains in the unit cell is too large, the number of available reflections is less, and hence the structure analysis was carried out in combination with the energy calculation argued below. In the present procedure, we first determined the molecular conformation by energy calculation and, on the basis of the conformation, found out the appropriate setting of

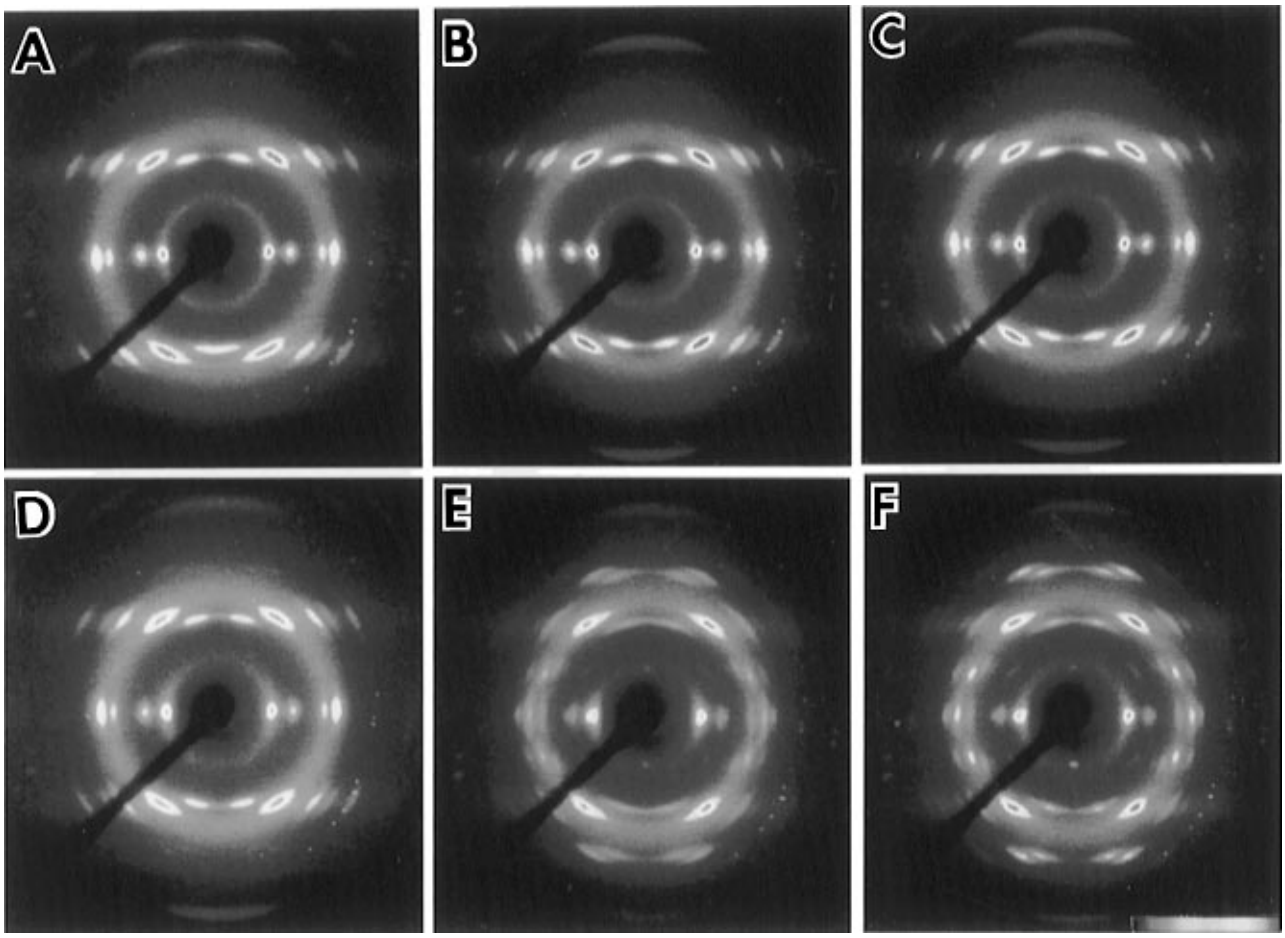

Figure 9. Changes of WAXPDs of iPVCH which was prepared by drawing at 130 °C and subsequently annealed at 250 °C. Individual patterns were taken with the present X-ray diffraction system while a constant stress was applied on the sample in the direction of the molecular axis at 133 °C during an exposure of 5 min: (A) no stress; (B) 5.5 MPa, (C) 9.4 MPa, (D) 12.8 MPa, (E) 15.0 MPa; (F) after stress is removed. All the patterns are photographed from the pictures which were displayed on a CRT in the form of the patterns of a cylindrical camera.

the chains in the unit cell, that is, the rotating angle of molecules around their molecular axis and the relative shift among them along the axis (the *c* axis direction), minimizing the discrepancy between the observed and calculated X-ray diffraction intensity data as usual. It is thus most probable that the molecular chains of 4/1 helical conformation should be arranged in the unit cell as shown in the projection on the basal plane in Figure 10. The coordinates of three successive, basic carbons thus obtained (arrowed in Figure 10) are shown in fractional coordinates: *a* {0.713, 0.201, 0.156}, *b* {0.732, 0.191, 0.380}, and *c* {0.799, 0.213, 0.406}. We are able to construct the conformation of the chains and dispose them in the unit cell by taking the symmetry operations. In the case of helical chains, there are two different types of chains in helical sense, i.e., right-handed (R) and left-handed (L). Further, we notice that since both types of helical chains are asymmetric with respect to the plane normal to the chain axis, there are two different alignments with respect to the *c* axis in the unit cell. However, the two different kinds of chains are uniquely disposed in the unit cell as in Figure 10 so that the symmetric requirements of the space group $I4_1/a$ are fulfilled (cf. Figure 1 in ref 2). Here it is to be noted that since the molecular conformation would be largely affected by intermolecular interactions, it is further necessary to refine the molecular conformation and crystal structure by taking the intermolecular energy into account. Refinement is in progress and will be reported elsewhere.

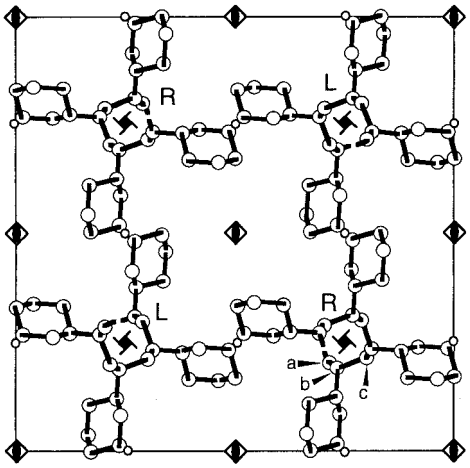

Figure 10. Packing of iPVCH chains of 4/1 helical conformation in the unit cell of Form I as a projection on the basal plane. The symmetry operations of space group of $I4_1/a$ are superposed. Open circles denote carbon atoms. The carbon−carbon bonds are drawn in bold lines. R and L mean the right- and left-handed chains, respectively. The coordinates of the carbons marked with a, b, and c are listed in the text.

Now, the conformation of a chain was expressed in terms of dihedral angles, τ_1, τ_2, and τ_3, as sketched in Figure 11. The potential energy of a single chain was computed as a function of these parameters. In computing the potential energy, other parameters such as bond angle and bond length are fixed to the values as

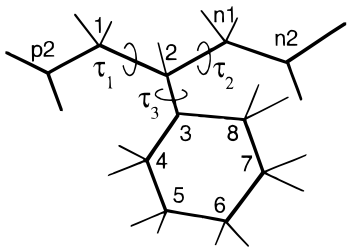

Figure 11. Parameters defining an iPVCH chain, which are needed in order to compute the potential energy of the single chain. Bold and thin lines are C−C and C−H bonds, respectively. The numbers are indices specifying the carbon atoms of a monomer unit and the characters n and p prior to the numbers designate the next and succeeding monomer units to the specified monomer unit, respectively. τ_1 is defined as the dihedral angle between the planes containing three successive carbons, C_{p2}, C_1, and C_2, and that of C_1, C_2, and C_{n1}. In the same way, τ_2 is the dihedral angle between planes of C_1, C_2, and C_{n1} and of C_2, C_{n1}, and C_{n2}, and τ_3 is between planes of C_1, C_2, and C_3 and of C_2, C_3, and C_4. In all cases, the angle of the *cis* conformation is defined as 0°.

Table 2. Bond Angles and Bond Lengths

atomic pair	bond length (Å)	bond angle (deg)
C−C	1.54	
C−H	1.09	
C−C−C		109.4
C−C−H		109.4

Table 3. Parameters of Lennard-Jones Potential of Various Atomic Pairs

atom combination	*A*	*B*
C−C	2.86×10^5	370
C−H	3.80×10^4	128
H−H	4.46×10^3	46.7

in Table 2. Further, the cyclohexyl groups are assumed to take the chair conformation, because it is normally more stable than the boat conformation. The following 6−12 type of potential function (Lennard-Jones potential function) was used as the potential function for a nonbonded atomic pair:

$$A/r_{ij}^{\,6} - B/r_{ij}^{\,12} \qquad (1)$$

where r_{ij} is the distance between the ith and jth atoms. Constants A and B for various atomic pairs are listed in Table 3. Figure 12 shows the contour map of the computed potential energy of a single chain as a function of τ_1 and τ_2. Figure 12 is drawn as follows: the potential energies are computed by changing τ_3 for the fixed τ_1 and τ_2 and the minimum value of them is selected. This process was iterated by changing the angles τ_1 and τ_2, and the thus selected values are plotted as a function of τ_1 and τ_2. The circle indicated by 4/1, drawn in Figure 12, means that whenever a chain has the dihedral angles τ_1 and τ_2 on the circle, it takes the 4/1 helical conformation irrespective of the values. On the other hand, the curves with $c' = 0.161$ nm implies that the projected displacement distance per monomer unit on the screw axis is 0.643/4 nm whenever a chain has the dihedral angles τ_1 and τ_2 on the curves. Thus, the crossing points of the curves ($c' = 0.161$ nm) and the circle (4/1) correspond to the Form I with a 4/1 helix of the repeating distance of 0.643 nm.[9] The chain conformation which has the dihedral angles τ_1 and τ_2 corresponding to the crossing points of the line and circle fulfill both requirements corresponding to real chains. There are four crossing points, but two of the four are found to be unstable from the energy map (Figure 12).

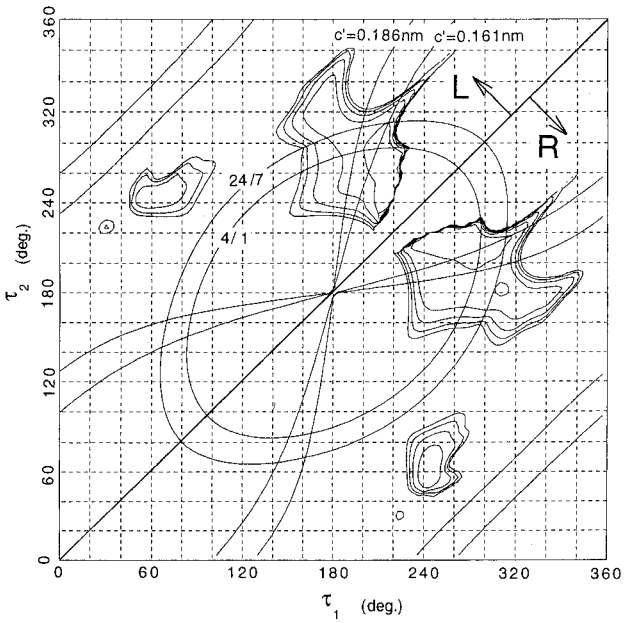

Figure 12. Potential map of a single iPVCH chain as a function of dihedral angles τ_1 and τ_2. Contour lines are drawn at an interval of 5 kcal/mol per monomer. Regions indicated by R and L correspond to the right- and left-handed helices, respectively. τ_1, τ_2, and τ_3 of the crossing points are listed in Table 4. c' is the projected displacement distance per monomer unit on the screw axis. $c' = 0.161$ nm corresponds to the 4/1 helix with $c = 0.643$ nm, and $c' = 0.186$ nm to the 24/7 helix with $c = 4.458$ nm.

Table 4. Crystallographic Constraints and the Corresponding Rotation Parameters

Form	helix	c' (nm)	τ_1 (deg)	τ_2 (deg)	τ_3 (deg)[a]
I	4/1	0.161	276	209	249
			209	279	232
II	24/7	0.186	290	198	57
			192	290	256

[a] Determined from energy minimum.

Thus, the remaining two in the valley of the potential map are supposed as preferable conformations and lead to only two kinds of conformation, R- and L-type, which correspond to the right- and left-handed helix of the main chain, respectively. The crystallographical demands make the two pairs of the two types of chains packed into a unit cell. Here, τ_3s in Table 4 give the minimum values of energy calculated by changing τ_3 for the chain skeleton corresponding to each crossing point. There seems to be no relation between τ_3s of R- and L-type at first glance of Table 4, but they are mutually in such a relation that chains hold a mirror conformation.

(2) Form II. It is shown that Form II has the chain conformation of a 24/7 helix.[3] In the same way as above, the circle corresponding to the 24/7 helix and the curves with the repeating distance $c' = 0.186$ (4.458/24) nm are added in the contour map of potential energy of Figure 12. Crossing points are still in the valley, and hence the chain conformation of Form II is stable although it is not so stable as that of Form I. However, since we observed reflections which are not explained on the basis of the present unit cell of Form II, giving a repeating distance longer than 4.458 nm, the chain conformation of the 24/7 helix is not considered to be the correct one at the present time. The structural analysis of Form II is in progress.

Here, we shall consider issue (3) in the first section: The broad halo in Figures 4A and 4B is strong and weak

in Figure 4C. As a possible, simple interpretation, it is considered that there are still noncrystalline domains in the samples for Figures 4A and 4C, recrystallizing after annealing at temperatures above 248 °C. It is to be noted, however, that halos are also caused by lattice defects of the first kind. Though the crystal structure of Form II is unresolved, it is clear that the orientation of the cyclohexyl groups in it is different from that in Form I with respect to the molecular axis. Further, we see that the valley of the potential is very broad so that a chain may have various types of chain conformations ranging from 4/1 to 24/7 or a more tight one. We guess also that it is most probable that the cyclohexyl groups might change their orientation part by part along the chain and that they might take the boat conformation partly. These irregularly oriented groups behave as point defects in the crystal structure and give rise to the diffuse halo. Further, as seen on the DSC curve of Figure 1, we shall notice here that tetrachloromethane can remain in iPVCH up to the second exothermic peak. The remaining tetrachloromethane may be incorporated solitarily in iPVCH as point defects or may cooperate to produce such a disorder of chains. In any way, iPVCH chains are ordered and rearranged to occupy the registered positions in the crystal structure when they are heated at high temperatures. This will be another reason why the strong amorphous halo of as-drawn samples becomes less intense by annealing. The as-drawn sample of Form I may have such a disordered crystalline structure and be less stable, and hence heat is evolved in the DSC curve A in Figure 3 when it is transformed into the ordered Form I by heat treatment. Actually, this idea is supported by the observation of run 5, that the sample never changes into another crystal structure by heating over the exothermic temperature of 248 °C.

Concluding Remarks

Though the crystal structure of Form II is not detailed, it is sure that the chain of Form II is more extended than that of Form I: in other words, chains are wrung tightly into a thin conformation. Though the different crystalline forms are observed depending on the drawing temperature when unoriented iPVCH is drawn, Form I is first produced independently of the drawing temperature, and then Form II is produced with further drawing. Thus, it is found that when the stress is imposed over the critical stress on the chain in the direction parallel to the chain axis, the chain is more extended. The critical stress depends on the temperature: 12.8 MPa at 133 °C and 9.3 MPa at 154 °C. Within the present experimental results, the lowest temperature where the stress-induced transformation from Form I to Form II takes place is about 110 °C. Inverse transformation from Form II to Form I occurs thermally at 248 °C, and the chain conformation becomes loose. The molecular mechanism of the "reversible" helix/helix transition will be made clear when the crystal structure of Form II is resolved.

Acknowledgment. We are most grateful to Drs. M. Kakugo and K. Watanabe of Sumitomo Chemical Co. Ltd. for supplying the samples, Prof. T. Ohta of Osaka City University for DSC−TG measurement, and Dr. T. Katayama of MAC Science Co. Ltd.

References and Notes

(1) Kakugo, M.; Watanabe, K. *Polym. Prepr. Jpn.* **1990**, *39*, 3884.
(2) Natta, G.; Corradini, P.; Bassi, I. W. *Makromol. Chem.* **1959**, *33*, 247.
(3) Noether, H. D. *J. Polym. Sci., Part C* **1967**, *16*, 725.
(4) Miyahara, J.; Takahashi, K.; Amemiya, Y.; Kamiya, N.; Satow, Y. *Nucl. Instrum. Methods Phys. Res.* **1986**, *A246*, 572.
(5) Amemiya, Y.; Wakabayashi, K.; Tanaka, H.; Ueno, Y.; Miyahara, J. *Science* **1987**, *237*, 164.
(6) Kawaguchi, A.; Murakami, S.; Katayama, K.; Mihoichi, M.; Ohta, T. *Bull. Inst. Chem. Res., Kyoto Univ.* **1991**, *69*, 145.
(7) Murakami, S.; Nishikawa, Y.; Tsuji, M.; Kawaguchi, A.; Kojiya, S.; Cakmak, M. *Polymer* **1995**, *36*, 291.
(8) Abe, A.; Hama, T. *J. Polym. Sci., Polym. Lett. Ed.* **1969**, *7*, 427.
(9) Miyazawa, T. *J. Polym. Sci.* **1961**, *55*, 215−231.

MA951789E